

Reentrant Non-Hermitian Skin Effect in Coupled Non-Hermitian and Hermitian Chains with Correlated Disorder

Jin Liu,^{1,*} Zhao-Fan Cai,^{1,*} Tao Liu,^{1,†} and Zhongmin Yang^{1,2,3,‡}

¹*School of Physics and Optoelectronics, South China University of Technology, Guangzhou 510640, China*

²*Research Institute of Future Technology, South China Normal University, Guangzhou 510006, China*

³*State Key Laboratory of Luminescent Materials and Devices and Institute of Optical Communication Materials, South China University of Technology, Guangzhou 510640, China*

(Dated: November 13, 2023)

The interplay of non-Hermiticity and disorder dramatically influences system's localization properties, giving rise to intriguing quantum phenomena. Although the intrinsic non-Hermitian skin effect (NHSE) is robust against the weak disorder even in a one-dimensional system, it becomes Anderson localization under strong disorder. Here, we study a localization-delocalization transition by coupling a strongly disordered Hatano-Nelson (HN) chain to a disordered Hermitian chain with its disorder correlated to that of HN chain. Regardless of the disorder strength, as the coupling strength between HN and Hermitian chain increases, a delocalization transition occurs. This leads to a reentrant NHSE due to the interplay of non-Hermiticity and correlated disorder. We reveal the underlying mechanism for the reentrant NHSE under correlated disorder. Moreover, the localization-delocalization transition is well captured by the real-space winding number.

Introduction.—Exotic physics of non-Hermitian systems has attracted considerable interest in recent years [1–27]. These systems include, but not limited to, classical optical systems with gain and loss [28–36], correlated electron systems as a result of finite-lifetime quasiparticles [37–39], and open quantum systems with post-selection measurements [40–42]. One of striking physical phenomena in non-Hermitian systems is the non-Hermitian skin effect (NHSE) [7–9, 43–53], where its bulk modes exhibit extensive sensitivity to the imposed boundary conditions. A majority of these bulk modes under periodic boundary conditions (PBCs) collapses into localized boundary modes in the open boundary conditions (OBCs), forming skin modes. These skin modes are rooted from intrinsic non-Hermitian topology [48, 49]. A lot of exciting non-Hermitian phenomena without their Hermitian counterparts are related to the NHSE, e.g., breakdown of conventional Bloch band theory [7], scale-free localization [21], and disorder-free entanglement phase transitions [26].

Disorders play a vital role in determining the behavior of Hermitian systems in various aspects including transport, entanglement and topology [54–57]. Very recently, the interplay of disorder and non-Hermiticity has been shown to give rise to a plethora of exotic phenomena [58–75], including nonunitary scaling rule of non-Hermitian localization, disorder-induced non-Bloch topological phase transitions and so on. Hatano and Nelson firstly investigated the non-Hermitian extension of the one-dimension Anderson model with the asymmetrical hopping [58], revealing the unexpected delocalization and appearance of skin modes for a weak random potential, while a one-dimensional Hermitian system is always localized [76]. This indicates that the non-Hermiticity can destroy Anderson localization. By further increasing disorder strength, all the states

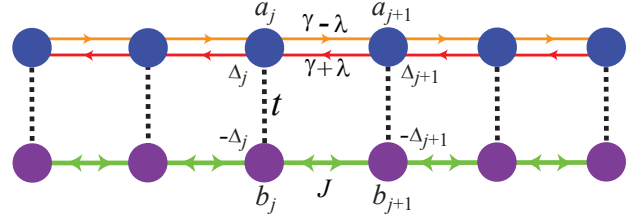


FIG. 1. A non-Hermitian Hatano-Nelson chain (top) with asymmetric hopping is coupled to a Hermitian chain model (bottom) with symmetric hopping. $\gamma \pm \lambda$ denote the asymmetric hopping strengths of the Hatano-Nelson chain, J is the symmetric hopping strength of the bottom chain, and t is the symmetric hopping strength of two chains. When the HN chain is subjected to strong random onsite potential Δ_j , the non-Hermitian skin-modes become Anderson-localized. While, the NHSE can be recovered if an anti-symmetric disorder is applied to the coupled Hermitian chain with the random onsite potential $-\Delta_j$.

remain localized. However, it remains unclear whether a localization to delocalization transition with the reentrant NHSE can be realized in a strong disordered non-Hermitian system.

In this Letter, we study a reentrant NHSE in coupled Hatano-Nelson (HN) and Hermitian chains with correlated disorder. Although the coupled chain is strongly disordered with random onsite potential applied to each chain, a delocalization transition occurs, accompanied by the reentrant NHSE, if the random onsite potential $\Delta_j^{(a)}$ in the HN chain is anti-symmetrically correlated to the random onsite potential $\Delta_j^{(b)}$ in the Hermitian chain, i.e., $\Delta_j^{(a)} = -\Delta_j^{(b)} = \Delta_j$. Even the disorder strength becomes ultra-large to cause the Anderson localization, the NHSE can be recovered by further increasing the coupling strength

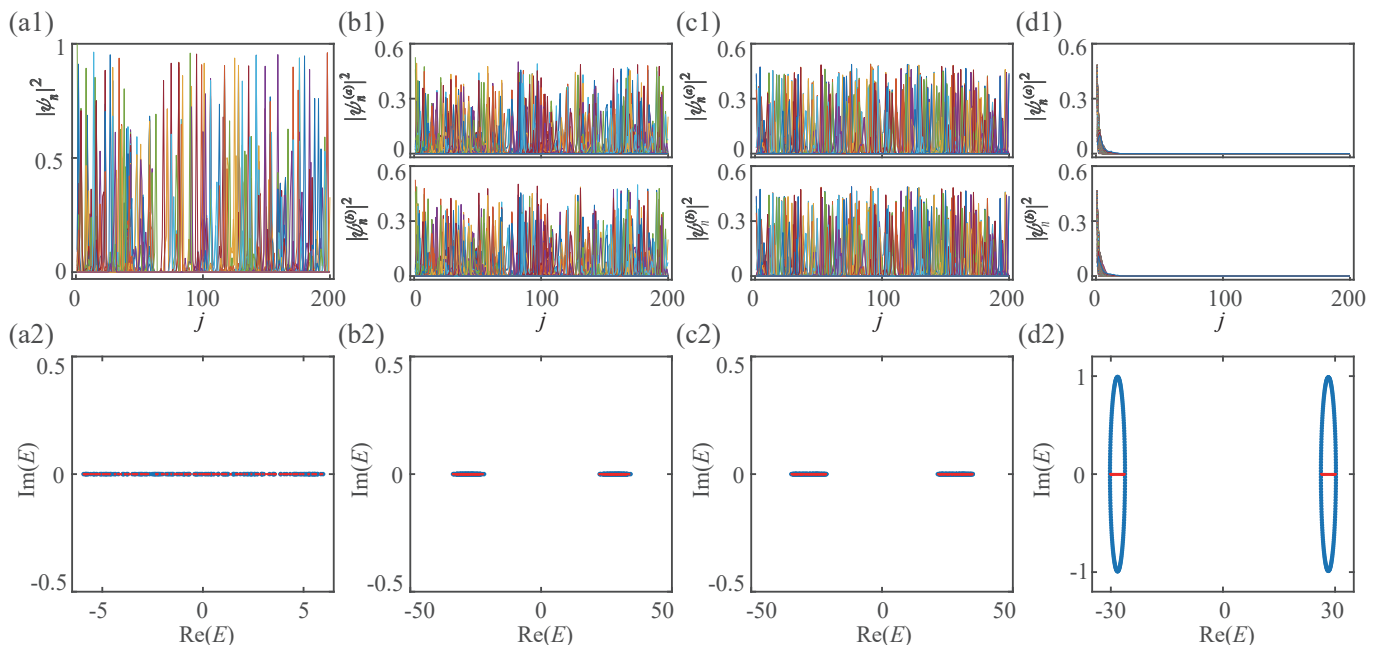


FIG. 2. (a1) Probability density distributions $|\psi_n(j)|^2$ of the HN single chain under strong onsite disorders, and (a2) the corresponding eigenenergies E in complex plan under PBC (blue dots) and OBC (red dots). (b1-d1) Probability density distributions $|\psi_n^{(a)}(j)|^2$ and $|\psi_n^{(b)}(j)|^2$ of the coupled chains subjected to uncorrelated random potential $\Delta_j^{(a)}$ and $\Delta_j^{(b)}$ (b1), symmetric random potential with $\Delta_j^{(a)} = \Delta_j^{(b)} = \Delta_j$ (c1), and anti-symmetric random potential with $\Delta_j^{(a)} = -\Delta_j^{(b)} = \Delta_j$ (d1). (b2-d2) are the corresponding corresponding eigenenergies in complex plan under PBC (blue dots) and OBC (red dots). The parameters used are $\gamma/J = \lambda/J = 1$, $W/J = 12$, $t/J = 28$, and $L = 200$.

between the HN and Hermitian chains. The underlying mechanism is intuitively analyzed, and the localization-delocalization phase transition is characterized by the real-space winding number.

Model.—We consider a 1D non-Hermitian Hatano-Nelson (HN) chain with asymmetric hopping [58], which shows a NHSE. When the HN chain is subjected to the random onsite potential, the interplay of non-reciprocal hopping and disorder can result in delocalization with partially extended single-particle eigenstates for weak disorder strength [58, 59, 61, 70]. While, a further increase of disorder strength leads to Anderson localization in the HN chain. In this work, we will show that the NHSE can be recovered even in the strong disorder by coupling the disordered HN chain to a disordered Hermitian chain with its disorder correlated to that in the HN chain, as shown in Fig. 1. The Hamiltonian of the hybrid system is written as

$$\begin{aligned} \mathcal{H} = & \sum_j \left[(\gamma + \lambda) a_j^\dagger a_{j+1} + (\gamma - \lambda) a_{j+1}^\dagger a_j \right] \\ & + \sum_j \left(J b_{j+1}^\dagger b_j + t a_j^\dagger b_j + \text{H.c.} \right) \\ & + \sum_j \left(\Delta_j^{(a)} a_j^\dagger a_j + \Delta_j^{(b)} b_j^\dagger b_j \right), \end{aligned} \quad (1)$$

where a^\dagger and b^\dagger are the particle creation operators for

the HN chain and the Hermitian chain, respectively, the asymmetric hopping is denoted by $\gamma \pm \lambda$, J is the symmetric hopping strength for the Hermitian chain, t is the coupling strength of two chains, and $\Delta_j^{(\mu)}$ ($\mu = a, b$) is the random onsite potential, applied to the HN chain ($\mu = a$) and the Hermitian chain ($\mu = b$), which is uniformly sampled in $[-W/2, W/2]$ with W being the disorder strength.

Reentrant NHSE.—Although the strong random onsite potential Δ_j leads to localization of all the states in the HN chain, we will show that a reentrant NHSE can occur if an anti-symmetric disorder scheme is applied to the coupled Hermitian chain with its random onsite potential being $-\Delta_j$. Figure 2 plots the probability density distributions of all the states under strong onsite disorder, and the corresponding complex eigenenergies under PBC (blue dots) and OBC (red dots). All the states in both the single HN chain and the coupled HN-Hermitian chains remain localized for the strong uncorrelated random onsite potential [see Fig. 2(a1,b1)]. The breakdown of NHSE is also indicated by the absence of point gap [see Fig. 2(a2,b2)].

We now consider two types of correlated disordered potential: symmetric disorder with $\Delta_j^{(a)} = \Delta_j^{(b)} = \Delta_j$, and anti-symmetric disorder with $\Delta_j^{(a)} = -\Delta_j^{(b)} = \Delta_j$, where Δ_j is randomly sampled in $[-W/2, W/2]$

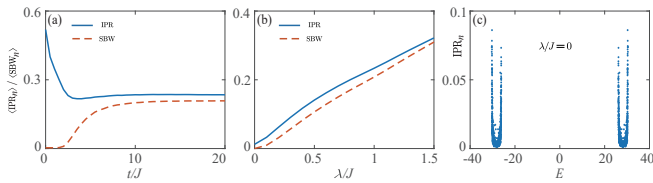


FIG. 3. Averaged IPR and SBW over all the eigenmodes (a) as a function of the coupling strength t with $W/J = 12$ and $\lambda/J = 1$, and (b) as a function of asymmetric hopping strength λ with $W/J = 12$ and $t/J = 28$ for the anti-symmetric random potential. (c) IPR_n vs. E for $\lambda/J = 0$. The other parameters are $\gamma/J = 1$, $\xi = 2$ and $L = 400$. The results are averaged over 1200 disorder realizations.

with zero expectation. For the symmetric and strong disordered potential, all the states are still localized [see Fig. 2(c1,c2)]. However, when the anti-symmetric and strong disorder is considered, the complex eigenspectrum (blue dots) in the PBC forms two point gaps for a large t , encircling the eigenenergies (red dots) in the OBC [Fig. 2(e)]. All the states inside the point gap localized at the left boundary, as shown in Fig. 2(d), where a reentrant NHSE occurs.

To further study the delocalization properties caused by the coupling strength t and the effect of asymmetric hopping λ , we calculate the inverse participation ratio (IPR) and skin-boundary weight (SBW) of each normalized eigenstate $\psi_n = (\psi_n^{(a)}, \psi_n^{(b)})^T$, which are defined as

$$\text{IPR}_n = \sum_j \left(|\psi_n^{(a)}(j)|^4 + |\psi_n^{(b)}(j)|^4 \right), \quad (2)$$

$$\text{SBW}_n = \sum_j \left(|\psi_n^{(a)}(j)|^4 + |\psi_n^{(b)}(j)|^4 \right) e^{-|j-j_c|/\xi}, \quad (3)$$

where the sums run over length L of the coupled chain, j_c denotes the site index of the left or right boundary, and ξ represents the exponentially decaying length from the boundary. $\text{IPR}_n \simeq 1/(2L)$ if the n th eigenstate ψ_n is extended, and drops to zero for an infinite system. In contrast, for eigenstates localized on N sites ($N \ll L$), $\text{IPR}_n \simeq 1/N$, and keeps finite for an infinite system. IPR cannot distinguish the skin-boundary modes from the Anderson-localized modes, while a finite SBW_n denotes the mode localized at the boundary (i.e., skin mode).

Figure 3(a) plots the averaged IPR and SBW over all the eigenmodes as a function of the coupling strength t for the disorder strength $W/J = 12$. This strong disordered potential causes Anderson localization for small t . As t increases, a delocalization occurs and skin modes appear, where all the modes are stayed in the boundary for large t [see also Fig. 2(d)]. By fixing the disorder and hopping strength W and t , we calculate the averaged IPR and SBW versus the asymmetric hopping

parameter λ , as shown in 3(b). For the Hermitian case with $\lambda = 0$, the anti-symmetric disorder induces the coexistence of localized and extended states [see also IPR_n in Fig. 3(c)] due to the finite size effect (Note that the anti-symmetric disorder cause all the modes localization in the long-size system for the Hermitian case.). As λ increase, a delocalization occurs, and all the states become skin modes for the strong nonreciprocal hopping with a large λ .

Physical mechanism.—To intuitively understand the physical mechanism of the reentrant NHSE for the strong inter-chain coupling under the anti-symmetric disorder, we consider the limited case with $|t| \gg |J|, |\gamma \pm \lambda|, |\Delta_j|$ for both symmetric and anti-symmetric disorders. In this case, the inter-chain hopping is dominant process, and we treat intra-chain hopping terms as perturbation. The Hamiltonian \mathcal{H} is thus decomposed as $\mathcal{H}_{\pm} = \mathcal{H}_{0,\pm} + \mathcal{V}$, with the unperturbed part reading

$$\mathcal{H}_{0,\pm} = \sum_j \left[t \left(a_j^\dagger b_j + \text{H.c.} \right) + \Delta_j \left(a_j^\dagger a_j \pm b_j^\dagger b_j \right) \right], \quad (4)$$

and perturbed part as

$$\begin{aligned} \mathcal{V} = & \sum_j \left[(\gamma + \lambda) a_j^\dagger a_{j+1} + (\gamma - \lambda) a_{j+1}^\dagger a_j \right] \\ & + \sum_j J \left(b_{j+1}^\dagger b_j + \text{H.c.} \right), \end{aligned} \quad (5)$$

where \mathcal{H}_+ denotes the coupled chains under the symmetric disorder effect, and \mathcal{H}_- under the anti-symmetric disorder effect.

For the strong inter-chain coupling limit with $|t| \gg |J|, |\gamma \pm \lambda|, |\Delta_j|$, $\mathcal{H}_{0,\pm}$ can be rewritten as

$$\mathcal{H}_{0,\pm} = \sum_{j,m=\pm} \xi_{\pm,j}^{(m)} \alpha_{m,j}^\dagger \alpha_{m,j}, \quad (6)$$

where $\alpha_{\pm,j} = (\pm a_j + b_j)/\sqrt{2}$, $\xi_{\pm,j}^{\pm} = \Delta_j \pm t$, and $\xi_{\pm,j}^{\mp} = \pm \sqrt{t^2 + \Delta_j^2}$. In the new basis $|\alpha_{\pm,j}\rangle = \alpha_{\pm,j}^\dagger |0\rangle$, we write \mathcal{H}_{\pm} as $\tilde{\mathcal{H}}_{\pm} = \mathcal{H}_{0,\pm} + \mathcal{H}_{\text{ladder}}$, with

$$\begin{aligned} \mathcal{H}_{\text{ladder}} = & \frac{J + \gamma + \lambda}{2} \sum_j \left(\alpha_{+,j}^\dagger \alpha_{+,j+1} + \alpha_{-,j}^\dagger \alpha_{-,j+1} \right) \\ & + \frac{J + \gamma - \lambda}{2} \sum_j \left(\alpha_{+,j+1}^\dagger \alpha_{+,j} + \alpha_{-,j+1}^\dagger \alpha_{-,j} \right) \\ & + \frac{J - \gamma - \lambda}{2} \sum_j \left(\alpha_{-,j}^\dagger \alpha_{+,j+1} + \alpha_{+,j}^\dagger \alpha_{-,j+1} \right) \\ & + \frac{J - \gamma + \lambda}{2} \sum_j \left(\alpha_{+,j+1}^\dagger \alpha_{-,j} + \alpha_{-,j+1}^\dagger \alpha_{+,j} \right). \end{aligned} \quad (7)$$

In Eq. (7), we have neglected the disorder in hopping terms, which is small for $|\Delta_j| \gg |J|, |\gamma \pm \lambda|$.

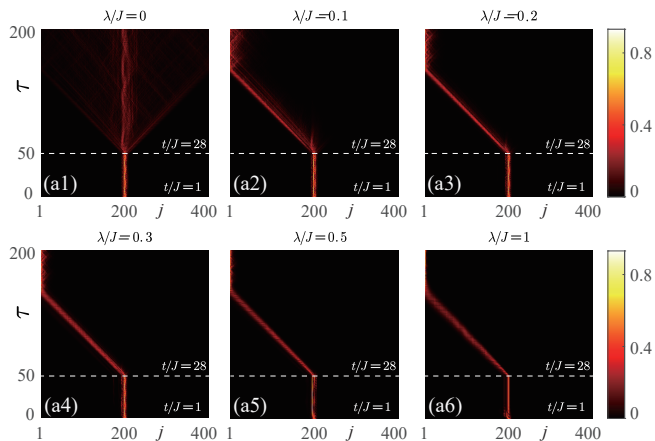


FIG. 4. Quenched dynamics of density distributions for different λ subjected to anti-symmetric disorder, where the initial state is set as the Gaussian wavepacket as $\psi_0(j) = \exp[-(j-j_0)^2/2\sigma^2]/\mathcal{N}$ centered at the site j_0 in the HN chain. At time $\tau = 50$, the hopping strength changes from $t/J = 1$ to $t/J = 28$. The parameters used are $\gamma/J = 1$, $W/J = 12$, and $L = 400$ with (a1) $\lambda/J = 0$, (a2) $\lambda/J = 0.1$, (a3) $\lambda/J = 0.2$, (a4) $\lambda/J = 0.3$, (a5) $\lambda/J = 0.5$, and (a6) $\lambda/J = 1$.

In the new basis, $\tilde{\mathcal{H}}_{\pm}$ describes a nonreciprocal Creutz ladder $\mathcal{H}_{\text{ladder}}$ [77] in the presence of disordered onsite potential $\mathcal{H}_{0,\pm}$ for symmetric and anti-symmetric disorder schemes, respectively. For the considered parameters in Fig. 2, $\mathcal{H}_{\text{ladder}}$ exhibits a NHSE with all the modes localized at the left boundary. Under the symmetric disorder scheme, the onsite random potential of the Creutz ladder is given by $\Delta_j \pm t$ for each chain, which leads to Anderson localization for strong disorder Δ_j . However, for the anti-symmetric disorder case, the onsite random potential of the ladder reads $\pm\sqrt{t^2 + \Delta_j^2}$ for each chain. Then, the disorder strength \tilde{W} of the Creutz ladder is $\tilde{W} < W^2/|8t|$. In the strong coupling limit with $|t| \gg |\Delta_j|$, i.e., $|t| \gg W$, the disorder strength \tilde{W} of the Creutz ladder is much smaller than the asymmetric hopping strength λ . Although an arbitrarily small amount of disorder leads to Anderson localization in the 1D Hermitian system [76], it has been shown that the interplay of non-Hermiticity and disorder causes Anderson transition [5, 58]. Therefore, the increasing hopping t eventually results in the reentrant non-Hermitian effects even for arbitrary disorder strength under the anti-symmetric disorder scheme.

Quenched dynamics.—The reentrant skin modes caused by the anti-symmetric disorder can be further manifested by studying the quenched evolution dynamics. The initial state is chosen as a Gaussian wavepacket as $\psi_0(j) = \exp[-(j-j_0)^2/2\sigma^2]/\mathcal{N}$ centered at the site j_0 , where \mathcal{N} is the normalization constant, and σ denotes the wavepacket width. The wavefunction at time τ is obtained by numerically calculating $\psi(j, \tau) =$

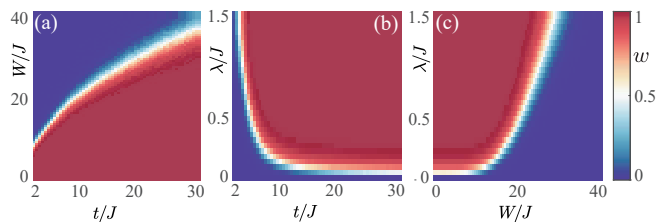


FIG. 5. Winding number w in the plane of (a) (W, t) with $\lambda/J = \gamma/J = 1$, (b) (λ, t) with $W/J = 12$, and (c) (λ, W) with $\gamma/J = 1$ and $t/J = 14$. The results are averaged over 1200 disorder realizations with $L = 200$.

$\exp(-i\mathcal{H}\tau)\psi_0(j)$. Figure 4 plots quenched dynamics of density distributions for different λ subjected to anti-symmetric disorder, where the hopping strength suddenly changes from $t/J = 1$ to $t/J = 28$ at time $\tau = 50$. For the Hermitian case with $\lambda/J = 0$ [see Fig. 4(a1)], the initial localized mode remains mostly localized after quench. The slight spreading of density distribution is attributed to finite size effect. While, as the asymmetric hopping parameter λ is considered and increases, the wavepacket initially localized at the center of the ladder becomes delocalized, and propagates towards the left boundary after quench, and it is finally localized at the boundary due to the interplay of NHSE and anti-symmetric disorder.

Phase diagram.—To characterize the localization to delocalization transition and appearance of non-Hermitian skin modes due to the interplay of anti-symmetric disorder, asymmetric hopping and coupling strength of two chains, we calculate the real-space winding number, which is defined as [67]

$$w(E_b) = \frac{1}{L'} \text{Tr}' \left(\hat{Q}^\dagger [\hat{Q}, \hat{X}] \right), \quad (8)$$

where \hat{Q} is positive-definite Hermitian matrix, which is obtained by the polar decomposition $(\mathcal{H} - E_b) = \hat{Q}\hat{P}$, with unitary matrix \hat{P} . \hat{Q} and \hat{P} are related to singular value decomposition $(\mathcal{H} - E_b) = \hat{M}\hat{S}\hat{N}^\dagger$, with $\hat{Q} = \hat{M}\hat{N}^\dagger$ and $\hat{P} = \hat{N}\hat{S}\hat{N}^\dagger$. \hat{X} is the coordinate operator, with $X_{jj',ss'} = j\delta_{j,j'}\delta_{s,s'}$ ($s = a, b$), and Tr' denotes the trace over the middle interval with length L' , where the whole chain is cut off from both ends. This definition of winding number avoids the effects from the system's boundary.

The phase diagrams, in the presence of anti-symmetric disorder, are shown in Fig. 5, and the phase boundary is clearly observed. Regardless of how large the disorder strength W is, we can infer that the skin modes reappear once the coupling strength t between the HN and Hermitian chains becomes large enough [see Fig. 5(a)]. Moreover, the phase boundary is strongly dependent on the asymmetric hopping strength λ [see Fig. 5(b,c)].

Conclusion and discussion.—In this work, we study the robust NHSE in the coupled HN and Hermitian chains in the presence of ultra-strong disorder. When

the strong random onsite potential is independently applied to each chain, the Anderson localization occurs. However, the Anderson transition takes places, accompanied by the reentrant NHSE when the random onsite potential in the HN chain is anti-symmetrically correlated to that in the Hermitian chain. We found that the sufficiently strong coupling strength between HN and Hermitian chain always leads to the reentrant non-Hermitian skin effect due to the interplay of non-Hermiticity and correlated disorder, no matter how strong the disorder is. This coupling-chain-induced NHSE can be manifested by the quenched dynamics in the strong disorder non-Hermitian system. Furthermore, the localization-delocalization transition is well captured by the real-space winding number.

The illustrated model can be realized in classical systems, including phononic and optical structures [78, 79], and electrical circuits [80, 81]. It can be also simulated in ultracold-atom systems [25, 82]. In the future, it is interesting to study the reentrant NHSE in disordered 2D non-Hermitian system, and also to consider the effects of interactions.

T.L. acknowledges the support from the Fundamental Research Funds for the Central Universities (Grant No. 2023ZYGXZR020), Introduced Innovative Team Project of Guangdong Pearl River Talents Program (Grant No. 2021ZT09Z109), National Natural Science Foundation of China (Grant No. 12274142), and the Startup Grant of South China University of Technology (Grant No. 20210012).

* These authors contributed equally

† E-mail: liutao0716@scut.edu.cn

‡ E-mail: yangzm@scut.edu.cn

- [1] V. V. Konotop, J. Yang, and D. A. Zezyulin, “Nonlinear waves in \mathcal{PT} -symmetric systems,” *Rev. Mod. Phys.* **88**, 035002 (2016).
- [2] T. E. Lee, “Anomalous edge state in a non-Hermitian lattice,” *Phys. Rev. Lett.* **116**, 133903 (2016).
- [3] D. Leykam, K. Y. Bliokh, C. Huang, Y. D. Chong, and F. Nori, “Edge modes, degeneracies, and topological numbers in non-Hermitian systems,” *Phys. Rev. Lett.* **118**, 040401 (2017).
- [4] Y. Xu, S. T. Wang, and L. M. Duan, “Weyl exceptional rings in a three-dimensional dissipative cold atomic gas,” *Phys. Rev. Lett.* **118**, 045701 (2017).
- [5] Z. Gong, Y. Ashida, K. Kawabata, K. Takasan, S. Higashikawa, and M. Ueda, “Topological phases of non-Hermitian systems,” *Phys. Rev. X* **8**, 031079 (2018).
- [6] R. El-Ganainy, K. G. Makris, M. Khajavikhan, Z. H. Musslimani, S. Rotter, and D. N. Christodoulides, “Non-Hermitian physics and \mathcal{PT} symmetry,” *Nat. Phys.* **14**, 11 (2018).
- [7] S. Yao and Z. Wang, “Edge states and topological invariants of non-Hermitian systems,” *Phys. Rev. Lett.* **121**, 086803 (2018).
- [8] S. Yao, F. Song, and Z. Wang, “Non-Hermitian Chern bands,” *Phys. Rev. Lett.* **121**, 136802 (2018).
- [9] T. Liu, Y.-R. Zhang, Q. Ai, Z. Gong, K. Kawabata, M. Ueda, and F. Nori, “Second-order topological phases in non-Hermitian systems,” *Phys. Rev. Lett.* **122**, 076801 (2019).
- [10] J. Y. Lee, J. Ahn, H. Zhou, and A. Vishwanath, “Topological correspondence between Hermitian and non-Hermitian systems: Anomalous dynamics,” *Phys. Rev. Lett.* **123**, 206404 (2019).
- [11] K. Kawabata, T. Bessho, and M. Sato, “Classification of exceptional points and non-Hermitian topological semimetals,” *Phys. Rev. Lett.* **123**, 066405 (2019).
- [12] Z. Y. Ge, Y. R. Zhang, T. Liu, S. W. Li, H. Fan, and F. Nori, “Topological band theory for non-Hermitian systems from the Dirac equation,” *Phys. Rev. B* **100**, 054105 (2019).
- [13] H. Zhou and J. Y. Lee, “Periodic table for topological bands with non-Hermitian symmetries,” *Phys. Rev. B* **99**, 235112 (2019).
- [14] H. Zhao, X. Qiao, T. Wu, B. Midya, S. Longhi, and L. Feng, “Non-Hermitian topological light steering,” *Science* **365**, 1163 (2019).
- [15] K. Kawabata, K. Shiozaki, M. Ueda, and M. Sato, “Symmetry and topology in non-Hermitian physics,” *Phys. Rev. X* **9**, 041015 (2019).
- [16] D. S. Borgnia, A. J. Kruchkov, and R.-J. Slager, “Non-Hermitian boundary modes and topology,” *Phys. Rev. Lett.* **124**, 056802 (2020).
- [17] T. Liu, J. J. He, T. Yoshida, Z.-L. Xiang, and F. Nori, “Non-Hermitian topological Mott insulators in one-dimensional fermionic superlattices,” *Phys. Rev. B* **102**, 235151 (2020).
- [18] L. Li, C. H. Lee, S. Mu, and J. Gong, “Critical non-Hermitian skin effect,” *Nat. Commun.* **11** (2020), 10.1038/s41467-020-18917-4.
- [19] Y. Ashida, Z. Gong, and M. Ueda, “Non-Hermitian physics,” *Adv. Phys.* **69**, 249 (2020).
- [20] T. Liu, J. J. He, Z. Yang, and F. Nori, “Higher-order Weyl-exceptional-ring semimetals,” *Phys. Rev. Lett.* **127**, 196801 (2021).
- [21] L. Li, C. H. Lee, and J. Gong, “Impurity induced scale-free localization,” *Commun. Phys.* **4** (2021), 10.1038/s42005-021-00547-x.
- [22] E. J. Bergholtz, J. C. Budich, and F. K. Kunst, “Exceptional topology of non-Hermitian systems,” *Rev. Mod. Phys.* **93**, 015005 (2021).
- [23] K. Zhang, Z. Yang, and C. Fang, “Universal non-Hermitian skin effect in two and higher dimensions,” *Nat. Commun.* **13** (2022), 10.1038/s41467-022-30161-6.
- [24] K. Li and Y. Xu, “Non-Hermitian absorption spectroscopy,” *Phys. Rev. Lett.* **129**, 093001 (2022).
- [25] Z. Ren, D. Liu, E. Zhao, C. He, K. K. Pak, J. Li, and G.-B. Jo, “Chiral control of quantum states in non-Hermitian spin-orbit-coupled fermions,” *Nat. Phys.* **18**, 385 (2022).
- [26] K. Kawabata, T. Numasawa, and S. Ryu, “Entanglement phase transition induced by the non-Hermitian skin effect,” *Phys. Rev. X* **13**, 021007 (2023).
- [27] K. Zhang, C. Fang, and Z. Yang, “Dynamical degeneracy splitting and directional invisibility in non-Hermitian systems,” *Phys. Rev. Lett.* **131**, 036402 (2023).
- [28] A. Regensburger, C. Bersch, M. A. Miri, G. Onishchukov, D. N. Christodoulides, and U. Peschel, “Parity-time

- synthetic photonic lattices,” *Nature* **488**, 167 (2012).
- [29] H. Jing, S. K. Özdemir, X. Y. Lü, J. Zhang, L. Yang, and F. Nori, “ \mathcal{PT} -symmetric phonon laser,” *Phys. Rev. Lett.* **113**, 053604 (2014).
- [30] H. Hodaei, M. A. Miri, M. Heinrich, D. N. Christodoulides, and M. Khajavikhan, “Parity-time-symmetric microring lasers,” *Science* **346**, 975 (2014).
- [31] B. Peng, Ş. K. Özdemir, F. Lei, F. Monifi, M. Gianfreda, G. L. Long, S. Fan, F. Nori, C. M. Bender, and L. Yang, “Parity-time-symmetric whispering-gallery microcavities,” *Nat. Phys.* **10**, 394 (2014).
- [32] L. Feng, Z. J. Wong, R. M. Ma, Y. Wang, and X. Zhang, “Single-mode laser by parity-time symmetry breaking,” *Science* **346**, 972 (2014).
- [33] B. Peng, Ş. K. Özdemir, S. Rotter, H. Yilmaz, M. Liertzer, F. Monifi, C. M. Bender, F. Nori, and L. Yang, “Loss-induced suppression and revival of lasing,” *Science* **346**, 328 (2014).
- [34] K. Kawabata, Y. Ashida, and M. Ueda, “Information retrieval and criticality in parity-time-symmetric systems,” *Phys. Rev. Lett.* **119**, 190401 (2017).
- [35] H. Lü, S. K. Özdemir, L. M. Kuang, F. Nori, and H. Jing, “Exceptional points in random-defect phonon lasers,” *Phys. Rev. Applied* **8**, 044020 (2017).
- [36] J. Zhang, B. Peng, Ş. K. Özdemir, K. Pichler, D. O. Krimer, G. Zhao, F. Nori, Y. X. Liu, S. Rotter, and L. Yang, “A phonon laser operating at an exceptional point,” *Nat. Photon.* **12**, 479 (2018).
- [37] H. Shen and L. Fu, “Quantum oscillation from in-gap states and non-Hermitian Landau level problem,” *Phys. Rev. Lett.* **121**, 026403 (2018).
- [38] T. Yoshida, R. Peters, and N. Kawakami, “Non-Hermitian perspective of the band structure in heavy-fermion systems,” *Phys. Rev. B* **98**, 035141 (2018).
- [39] Y. Nagai, Y. Qi, H. Isobe, V. Kozii, and L. Fu, “DMFT reveals the non-Hermitian topology and Fermi arcs in heavy-fermion systems,” *Phys. Rev. Lett.* **125**, 227204 (2020).
- [40] K. Yamamoto, M. Nakagawa, K. Adachi, K. Takasan, M. Ueda, and N. Kawakami, “Theory of non-Hermitian fermionic superfluidity with a complex-valued interaction,” *Phys. Rev. Lett.* **123**, 123601 (2019).
- [41] M. Naghiloo, M. Abbasi, Yogesh N. Joglekar, and K. W. Murch, “Quantum state tomography across the exceptional point in a single dissipative qubit,” *Nat. Phys.* **15**, 1232 (2019).
- [42] M. Nakagawa, N. Tsuji, N. Kawakami, and M. Ueda, “Dynamical sign reversal of magnetic correlations in dissipative Hubbard models,” *Phys. Rev. Lett.* **124**, 147203 (2020).
- [43] F. K. Kunst, E. Edvardsson, J. C. Budich, and E. J. Bergholtz, “Biorthogonal bulk-boundary correspondence in non-Hermitian systems,” *Phys. Rev. Lett.* **121**, 026808 (2018).
- [44] F. Song, S. Yao, and Z. Wang, “Non-Hermitian skin effect and chiral damping in open quantum systems,” *Phys. Rev. Lett.* **123**, 170401 (2019).
- [45] K. Yokomizo and S. Murakami, “Non-Bloch band theory of non-Hermitian systems,” *Phys. Rev. Lett.* **123**, 066404 (2019).
- [46] C. H. Lee and R. Thomale, “Anatomy of skin modes and topology in non-Hermitian systems,” *Phys. Rev. B* **99**, 201103 (2019).
- [47] K. Kawabata, M. Sato, and K. Shiozaki, “Higher-order non-Hermitian skin effect,” *Phys. Rev. B* **102**, 205118 (2020).
- [48] K. Zhang, Z. Yang, and C. Fang, “Correspondence between winding numbers and skin modes in non-Hermitian systems,” *Phys. Rev. Lett.* **125**, 126402 (2020).
- [49] N. Okuma, K. Kawabata, K. Shiozaki, and M. Sato, “Topological origin of non-Hermitian skin effects,” *Phys. Rev. Lett.* **124**, 086801 (2020).
- [50] F. Roccati, “Non-Hermitian skin effect as an impurity problem,” *Phys. Rev. A* **104**, 022215 (2021).
- [51] D. Halder, S. Ganguly, and S. Basu, “Properties of the non-hermitian SSH model: role of symmetry,” *J. Phys.: Condens. Matter* **35**, 105901 (2022).
- [52] S. Longhi, “Non-Hermitian skin effect and self-acceleration,” *Phys. Rev. B* **105**, 245143 (2022).
- [53] N. Okuma and M. Sato, “Non-Hermitian topological phenomena: A review,” *Annu. Rev. Condens. Matter Phys.* **14**, 83 (2023).
- [54] P. W. Anderson, “Absence of diffusion in certain random lattices,” *Phys. Rev.* **109**, 1492 (1958).
- [55] P. A. Lee and T. V. Ramakrishnan, “Disordered electronic systems,” *Rev. Mod. Phys.* **57**, 287 (1985).
- [56] E. J. Meier, F. A. An, A. Dauphin, M. Maffei, P. Massignan, T. L. Hughes, and B. Gadway, “Observation of the topological Anderson insulator in disordered atomic wires,” *Science* **362**, 929 (2018).
- [57] D. A. Abanin, E. Altman, I. Bloch, and M. Serbyn, “Colloquium: Many-body localization, thermalization, and entanglement,” *Rev. Mod. Phys.* **91**, 021001 (2019).
- [58] N. Hatano and D. R. Nelson, “Localization transitions in non-Hermitian quantum mechanics,” *Phys. Rev. Lett.* **77**, 570 (1996).
- [59] N. Hatano and D. R. Nelson, “Non-Hermitian delocalization and eigenfunctions,” *Phys. Rev. B* **58**, 8384 (1998).
- [60] J. Feinberg and A. Zee, “Non-Hermitian localization and delocalization,” *Phys. Rev. E* **59**, 6433 (1999).
- [61] Z. Gong, Y. Ashida, K. Kawabata, K. Takasan, S. Higashikawa, and M. Ueda, “Topological phases of non-Hermitian systems,” *Phys. Rev. X* **8**, 031079 (2018).
- [62] H. Jiang, L.-J. Lang, C. Yang, S.-L. Zhu, and S. Chen, “Interplay of non-Hermitian skin effects and Anderson localization in nonreciprocal quasiperiodic lattices,” *Phys. Rev. B* **100**, 054301 (2019).
- [63] C. Wang and X. R. Wang, “Level statistics of extended states in random non-Hermitian Hamiltonians,” *Phys. Rev. B* **101**, 165114 (2020).
- [64] S. Longhi, “Topological phase transition in non-Hermitian quasicrystals,” *Phys. Rev. Lett.* **122**, 237601 (2019).
- [65] A. F. Tzortzakakis, K. G. Makris, and E. N. Economou, “Non-Hermitian disorder in two-dimensional optical lattices,” *Phys. Rev. B* **101**, 014202 (2020).
- [66] D.-W. Zhang, L.-Z. Tang, L.-J. Lang, H. Yan, and S.-L. Zhu, “Non-Hermitian topological Anderson insulators,” *Sci. China Phys. Mech.* **63** (2020), 10.1007/s11433-020-1521-9.
- [67] J. Claes and Taylor L. Hughes, “Skin effect and winding number in disordered non-Hermitian systems,” *Phys. Rev. B* **103**, L140201 (2021).
- [68] X. Luo, T. Ohtsuki, and R. Shindou, “Universality classes of the Anderson transitions driven by non-

- Hermitian disorder,” *Phys. Rev. Lett.* **126**, 090402 (2021).
- [69] X. Luo, T. Ohtsuki, and R. Shindou, “Transfer matrix study of the Anderson transition in non-Hermitian systems,” *Phys. Rev. B* **104**, 104203 (2021).
- [70] K. Kawabata and S. Ryu, “Nonunitary scaling theory of non-Hermitian localization,” *Phys. Rev. Lett.* **126**, 166801 (2021).
- [71] K.-M. Kim and M. J. Park, “Disorder-driven phase transition in the second-order non-Hermitian skin effect,” *Phys. Rev. B* **104**, L121101 (2021).
- [72] C. C. Wanjura, M. Brunelli, and A. Nunnenkamp, “Correspondence between non-Hermitian topology and directional amplification in the presence of disorder,” *Phys. Rev. Lett.* **127**, 213601 (2021).
- [73] S. Weidemann, M. Kremer, S. Longhi, and A. Szameit, “Coexistence of dynamical delocalization and spectral localization through stochastic dissipation,” *Nat. Photon.* **15**, 576 (2021).
- [74] Q. Lin, T. Li, L. Xiao, K. Wang, W. Yi, and P. Xue, “Observation of non-Hermitian topological Anderson insulator in quantum dynamics,” *Nat. Commun.* **13** (2022), 10.1038/s41467-022-30938-9.
- [75] H. Liu, M. Lu, Z.-Q. Zhang, and H. Jiang, “Modified generalized Brillouin zone theory with on-site disorder,” *Phys. Rev. B* **107**, 144204 (2023).
- [76] E. Abrahams, P. W. Anderson, D. C. Licciardello, and T. V. Ramakrishnan, “Scaling theory of localization: Absence of quantum diffusion in two dimensions,” *Phys. Rev. Lett.* **42**, 673 (1979).
- [77] M. Creutz, “End states, ladder compounds, and domain-wall fermions,” *Phys. Rev. Lett.* **83**, 2636 (1999).
- [78] K. Wang, A. Dutt, K. Y. Yang, C. C. Wojcik, J. Vučković, and S. Fan, “Generating arbitrary topological windings of a non-Hermitian band,” *Science* **371**, 1240 (2021).
- [79] Q. Zhou, J. Wu, Z. Pu, J. Lu, X. Huang, W. Deng, M. Ke, and Z. Liu, “Observation of geometry-dependent skin effect in non-Hermitian phononic crystals with exceptional points,” *Nat. Commun.* **14** (2023), 10.1038/s41467-023-40236-7.
- [80] T. Helbig, T. Hofmann, S. Imhof, M. Abdelghany, T. Kiessling, L. W. Molenkamp, C. H. Lee, A. Szameit, M. Greiter, and R. Thomale, “Generalized bulk–boundary correspondence in non-Hermitian topoelectrical circuits,” *Nat. Phys.* **16**, 747 (2020).
- [81] D. Zou, T. Chen, W. He, J. Bao, C. H. Lee, H. Sun, and X. Zhang, “Observation of hybrid higher-order skin-topological effect in non-Hermitian topoelectrical circuits,” *Nat. Commun.* **12** (2021), 10.1038/s41467-021-26414-5.
- [82] Q. Liang, D. Xie, Z. Dong, H. Li, H. Li, B. Gadway, W. Yi, and B. Yan, “Dynamic signatures of non-Hermitian skin effect and topology in ultracold atoms,” *Phys. Rev. Lett.* **129**, 070401 (2022).